Peer-reviewed version available at *Materials* **2019**, *12*, 305; doi:10.3390/ma12020305

Article

A comparison of ethylene tar-derived isotropic pitches prepared by air blowing and nitrogen distillation method and their carbon fibers

Kui Shi [1,2], Jianxiao Yang [1,2,*], Chong Ye [1,2], Hongbo Liu [1,2] and Xuanke Li [1,2,*]

[1] College of Materials Science and Engineering, Hunan University, Changsha, Hunan 410082, China
[2] Hunan Province Key Laboratory for Advanced Carbon Materials and Applied Technology, Hunan University, China
Kui Shi: skhnu123@163.com
Jianxiao Yang: yangjianxiao@hnu.edu.cn
Chong Ye: 15874950624@163.com
Hongbo Liu: hndxlhb@163.com
Xuanke Li: xuankeli@hnu.edu.cn
[*] Correspondence: yangjianxiao@hnu.edu.cn; Tel.: +86-1521-100-5929 (Jianxiao Yang)

xuankeli@hnu.edu.cn; Tel.: +86-1599-427-9703 (Xuanke Li)

Abstract: Two isotropic pitches were prepared by air blowing and nitrogen distillation method using ethylene tar (ET) as a raw material. And correspondent carbon fibers were obtained through conventional melt spinning, stabilization and carbonization. The structures and properties of resultant pitches and fibers were characterized and their differences were discussed in this work. The results showed that introduction of the oxygen by air blowing method could quickly increase the yield and softening point of pitch. Moreover, the air blown pitch (ABP) composed of linear methylene chains of aromatic molecules while the nitrogen distilled pitch (NDP) mainly contained polycondensed aromatic rings, which was due to the oxygen containing functional groups existed in ABP could impede order stack of pitch molecules and form methylene bridge structure, instead of aromatic condensed structure like NDP. Meanwhile, the spinnability of ABP was not decreased even containing 2.31 wt% oxygen. In contrast, ABP had narrower molecular weight distribution, which contributed to better stabilization properties and higher tensile strength of carbon fiber. The tensile strength of carbon fibers from ABP was reached to 860 MPa with fiber diameter of about 10 μm, which was higher than that of NDP-derived carbon fibers of 640 MPa.

Keywords: Carbon fiber; ethylene tar; isotropic pitch; air blowing

1. Introduction

Carbon fibers (CFs) are widely used in military, industrial and sports because of their high mechanical properties, low density and good conductive properties [1]. Recently, the raw materials of pitch-based CFs are usually coal or petroleum derived by-products, which are abundant, low cost and have high carbonization yield [2, 3]. Therefore, more and more researchers are pursuing low-cost pitch-based CF because of its considerable advantage in price and extensive application prospects in the fields of automobile, sporting goods, building materials, C/C composites, activated carbon fibers, thermal field etc [4-9]. Therefore, a lot of raw materials and preparation methods of pitch precursor have been tried, including bromination and subsequent dehydrobromination of naphtha-cracked oil [3], tailored suitable molecular weight portion from Hyper-coal by methylnaphthalene [10], and heat treatment of pyrolyzed fuel oil [11], and so on. In our experiment, Ethylene tar (ET) is the by-product of ethylene production, which is rich in resources, low cost and low ash content compared to other precursors especially coal tar pitch which usually contains primary quinoline insoluble that need to be removed firstly. Therefore, ET is expected to be an ideal raw material for preparing the spinnable pitch. In addition, atmospheric distillation and air blowing are the most commonly methods to prepare spinnable pitch for CFs production [12-16]. Compared to atmospheric distillation which mainly consists the removal of light composition and condensation polymerization of heavy composition during the reaction, air blowing is recognized as an effective method to increase the softening point (SP) and the yield of pitch because oxidation can link molecules through methylene formed by oxidative dehydrogenation of aliphatic side chains or oxygen-containing functional groups as bridge like C-O-C and C=O formed by oxidation of aliphatic side chains [12, 15, 17], meanwhile suppress the formation of mesophase for obtaining homogenous pitch [18]. However, many researchers mainly focused on the different properties of pitch from different raw materials and preparation method. Most of them ignored the evolution and influence of oxygen during the preparation process of pitch-based CFs by air blowing method [19-21]. Actually, we should focus on the oxygen existed in pitch precursor may lead different molecular structure, and the corresponding molecular structure of pitch would impact on the spinnability of pitch and stabilization and carbonization process of pitch fiber. Meanwhile, we proposed that the appropriate introduced oxygen in pitch precursor could improve the mechanical properties of resultant carbon fibers prepared at the low carbonization temperature below 1200°C due to the introduced oxygen in pitch precursor was more stable than the introduced oxygen from stabilization process.

Therefore, in this work, two kinds of ET-derived isotropic pitches were prepared by nitrogen distillation and air blowing method in order to compare the difference of their molecular structures and clarify the difference and influence of oxygen introduced during the preparation of pitch precursor or during the stabilization process of pitch fibers on the properties of the corresponding CFs.

2. Materials and Methods

2.1 Materials

ET was supplied from Wuhan Luhua yueda chemical co. LTD, China. The ET was used as a raw material for preparation of spinnable pitch, which is completely soluble in toluene.

2.2 Preparation of spinnable pitches

The air blown pitch (ABP) was prepared by the air blowing method as follows: (1) The ET was distilled at 250°C in a 2 L stainless steel reactor to remove the light components to obtain basic pitch. (2) The basic pitch was air blown at 280°C for 3 h in the 3 L/min air mood to attain oxidized pitch. (3) In order to get the spinnable pitch with high SP, the oxidized pitch was further heat treated at 350°C for 4 h in the 3 L/min N_2 mood. For comparison, the nitrogen distilled pitch (NDP) with almost the same SP was prepared by heating ET at 380°C for 5h in the 3L/min nitrogen atmosphere.

2.3 Preparation of carbon fibers

The prepared NDP and ABP were spun into pitch fibers (PFs) at a temperature equal to their SP + 80°C using a melt spinning method with a single-hole spinneret (diameter = 0.2 mm, length/diameter = 3). For this procedure, a laboratory spinning apparatus was used with a nitrogen pressure of 0.4 MPa and winding speeds of 300-500 rpm (100 rpm=60 m/min) to get the pitch fibers with different diameter, respectively. The spun PFs were stabilized by heating from room temperature to 280°C with a rate of 0.5°C/min, holding at this temperature for 1 h with an air flow of 500 mL/min. Then the stabilized fibers (SFs) were successively carbonized at 1200°C for 30 min at a heating rate of 5°C/min with a nitrogen flow rate of 100 mL/min. The resultant spun PFs, SFs and CFs from NDP and ABP were labeled as NDP-PF, ABP-PF, NDP-SF, ABP-SF, NDP-CF and ABP-CF, respectively.

2.4 Characterization of pitches and carbon fibers

The SP of pitch was determined by a CFT-100EX capillary rheometer (Shimadzu). The solubility of pitch in *n*-hexane, toluene and quinoline was determined using Soxhlet extraction method to obtain the *n*-hexane soluble (HS), *n*-hexane insoluble and toluene soluble (HI-TS), toluene insoluble and quinoline soluble (TI-QS) and quinoline insoluble (QI) fractions. Carbon, hydrogen, sulfur and nitrogen contents were determined with a Elementar Vario EL III elemental analyzer (Elementar). The oxygen content was obtained by the subtracting method (O=100-C-H-N-S). Fourier transform infrared (FT-IR) spectra were obtained using KBr disc technique (sample/KBr=1/100) in a Nicolet iS10

Peer-reviewed version available at Materials 2019, 12, 305; doi:10.3390/ma12020305

FT-IR spectrometer (Thermo Fisher Scientific). Each spectrum was an average of 32 scans with a resolution of 4 cm^{-1}. Solution state ^{13}C nuclear magnetic resonance (^{13}C-NMR) spectra were obtained using a Bruker 600MHz Advance NMR spectrometer (Bruker). The quantitative ^{13}C spectra were recorded by dissolving samples in *d*-chloroform ($CDCl_3$) solvent (sample/$CDCl_3$=100 mg/1 mL) with tetramethylsilane used as chemical shift reference. The ^{13}C-NMR spectra were quantitatively analyzed by the ratio of the peak integral area. X-Ray diffraction (XRD) analyses were performed by a D8 Advance diffractometer (Bruker) with Cu Kα radiation (λ=0.15406 nm) generated at 32 kV and 50 mA with scan speed of 1°/min for 2 theta values between 5 and 80°. The thermogravimetric (TG) properties of samples were measured using a STA 449 F5 thermal analyzer (Netzsch). The thermal stability and coking value (CV) yield of obtained pitches were analyzed in 40 mL/min nitrogen moon with a heating rate of 5°C/min to 900°C. Meanwhile, to evaluate the stabilization properties of spun PFs, the obtained PFs were also analyzed by TG with different heating rates (0.5°C/min, 1°C/min, 2°C/min, 4°C/min) to 600°C in the 40 mL/min air moon for finding their maximum weight gain (W_{max}) and corresponding maximum temperature (T_{max}) and calculating their reaction activation energy (E_a). Moreover, the gas released off during carbonization of PFs and SFs were measured by Hiden Analytical HAS-301-1474 mass spectrometer (MS) (Hiden Analytical) coupled with TG from 20 to 1200°C with a rate of 10°C/min and an Argon flow 20mL/min, the MS was performed at RGA mode with a SEM detector and the quartz capillary connected to thermal analyzer was heated to 160°C. The morphologies and the diameter of the CFs were observed by JSM-6700F field emission scanning electron microscopy (SEM) (JEOL) with 5 kV. Tensile strength and Young's modulus of CFs were measured at room temperature using mono-filaments with a gauge length of 20 mm. The diameter of CFs was observed by SEM after tensile experiment. Tensile strength and Young's modulus were evaluated from the mean value of 30 tests, the values distributing within 10%.

3. Results and discussion

3.1. Characterization of NDP and ABP

The general characteristics of pitches were summarized in Table 1. The yield of ABP was higher than that of NDP even their SP were almost the same. This result was in line with other results from previous researchers, which was due to the air blowing method could increase SP more quickly [17]. It was apparent that air blowing brought large amount of oxygen into the pitch, as the oxygen content of ABP was up to 2.31%, higher than NDP which was 0.78%. Compared to ET, the solubility of NDP and ABP in *n*-hexane and toluene decreased, HI-TS increased from 48.4% for ET to 59.8% and 83.2% for NDP and ABP respectively as shown in Fig. 1. It should be noted that TI appeared in both NDP and ABP, but the TI of NDP was larger than ABP, and QI appeared in NDP, which declared that the nitrogen distillation method was more effective to accelerate polymerization reaction and was easier to form the larger molecular than air blowing method [22]. This also could be confirmed by larger C/H atoms rate of NDP than the ABP, which were 1.40 and 1.26, respectively. Although NDP had more large molecules, it was believed that the molecular weight distribution of ABP was narrower and more uniform than NDP from its quite high HI-TS. The SP of ABP was equal to that of NDP even at lower treatment temperature because of that larger molecules were produced through oxidative cross-linking of small molecules when air blowing. Meanwhile, oxidation linking suppressed the molecule aggregating and uneven polymerization happened in nitrogen distillation process. This more homogeneous composition of ABP would be beneficial to its spinning performance.

Peer-reviewed version available at *Materials* **2019**, *12*, 305; doi:10.3390/ma12020305

Table 1. General properties of pitches.

Samples	SP (^oC)	Yield (%)	Elemental analysis (%)					
			C	H	N	S	O	C/H
NDP	253	22	93.53	5.56	0.02	0.04	0.78	1.40
ABP	252	28	91.55	6.06	0.05	0.10	2.31	1.26

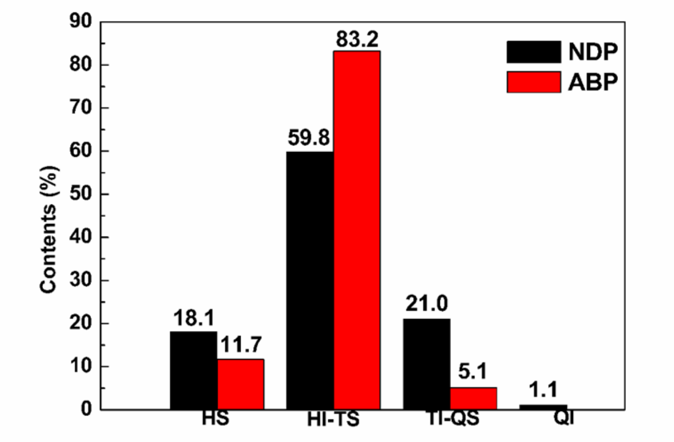

Fig. 1 Solubility parameter of NDP and ABP

FT-IR analysis shown in Fig. 2 was carried out to verify the functional group in NDP and ABP. The absorption peaks at 3050 cm^{-1} and 1600 cm^{-1} were assigned to the presence of aromatic C-H and aromatic C-C stretching, respectively. The stronger absorbance at 2920 cm^{-1} and 2850 cm^{-1} in ABP correspond to methylene hydrogen asymmetric and symmetric stretching, respectively [23]. The peak at 1450 cm^{-1} corresponding to methylene hydrogen bending was clearly stronger in intensity. The broad peak at 3300-3600 cm^{-1} might be ascribed to hydroxyl of H_2O in the pitch [24]. It must also be mentioned that new peak appeared at 1700 cm^{-1} of ABP compared to NDP, which was assigned to C=O stretching vibration. This could be easily explained by higher oxygen content of ABP as shown in Table 1. Another weak bond at 1260 cm^{-1} belonging to C-O stretching could also be observed. The emergence of oxygen containing functional groups indicated that oxygen may connect pitch molecules as oxygen bridge by air blowing.

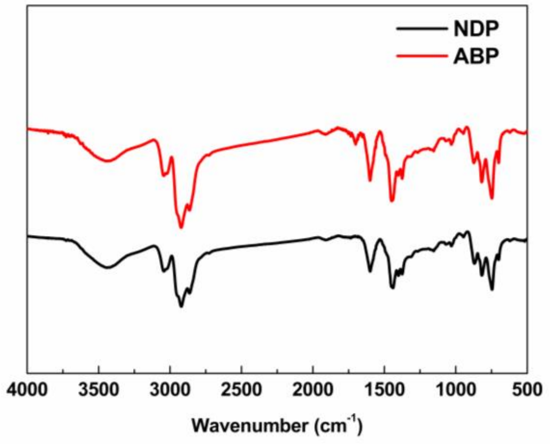

Fig. 2 FT-IR spectra of NDP and ABP

In order to further study the molecular structure of NDP and ABP, ^{13}C-NMR was performed. The ^{13}C-NMR spectra of NDP and ABP were plotted in Fig. 3. The normalized integration data of ^{13}C-NMR spectra was presented in Table 2. Larger aromaticity of NDP could be demonstrated by larger C_{ar}/C_{al} than ABP, which was 5.29 and 2.85, respectively. Most of the aromatic carbon in NDP was $C_{ar1,3}$, suggested abundant pericondensed structure in NDP [25]. This result indicated more condensed large molecules in NDP produced by heat treatment, which was reflected by higher insoluble substance content shown in Fig. 1. More aliphatic carbon in ABP than NDP existed in the form of CH_2 and $C_{\alpha2}$, indicated more methylene bridge structures in ABP formed by oxidative dehydrogenation，which was in accordance with the above analysis.

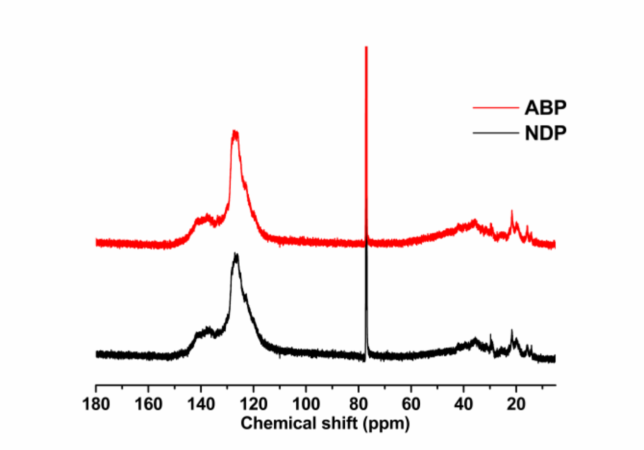

Fig. 3 ^{13}C-NMR spectra of NDP and ABP

Table 2. Normalized integration data based on the solid ^{13}C NMR spectra.

Samples	C_{al}			C_{ar}		C_{al}	C_{ar}	C_{ar}/C_{al}
	CH_3	CH_2	$C_{\alpha2}$	$C_{ar1,3}$	$C_{ar1,2}$			
NDP	0.04	0.08	0.04	0.60	0.24	0.16	0.84	5.29
ABP	0.03	0.14	0.09	0.52	0.22	0.26	0.74	2.85

CH_3, methyl carbon; CH_2, methylene (CH_2) carbon α or further from an aromatic ring in free side chain; $C_{\alpha2}$, CH_2 carbon in bridge/hydroaromatic structures; $Car_{1,3}$, pericondensed aromatic carbon (C_{ar3}) and protonated aromatic carbon (CH_{ar}); $Car_{1,2}$, catacondensed aromatic carbon, aromatic carbon both with heteroatomic or aromatic substituents (C_{ar2}), and the region correspondent to aromatic carbon joined to aliphatic chains; C_{al}, total aliphatic carbon; C_{ar}, total aromatic carbon.

Fig. 4 showed XRD graph of the NDP and ABP. Both of them showed broad peak between 10 and 30°. Peaks between 10 and 20° were attributable to asphaltene components while those between 20 and 30° were attributable to stacked molecular structures [26]. Therefore, the stacked structure was more evident in the NDP than in the ABP due to the larger condensed aromatic molecules in NDP as shown in Fig 1. In contrast, oxygen existed in ABP impeded order stack of molecules. Nevertheless, more symmetrical peak of ABP may indicate more uniform composition, which was consistent with extraordinarily uniform components presented in Fig 1.

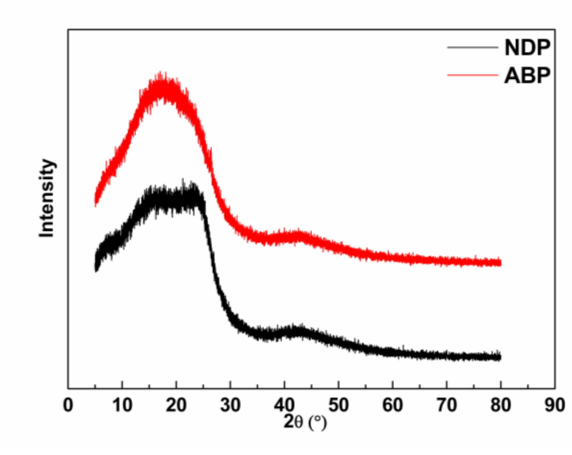

Fig. 4 X-ray diffractograms of NDP and ABP

Peer-reviewed version available at Materials 2019, 12, 305; doi:10.3390/ma12020305

3.2. Spinning properties of NDP and ABP

The viscosity-temperature curves of NDP and ABP were shown in Fig. 5. The viscosity of both NDP and ABP decreased sharply as increasing the temperature when the temperature was lower than 310°C, while the viscosity-temperature curves became almost flat above 330°C. because of temperature sensitive property of pitch, then gradually to about 330°C. It was noticed that the viscosity-temperature curve of ABP showed two jumping steps during the 310°C to 330°C, which suggested that the ABP had worse spinning performance than the NDP. However, both of them had excellent spinning performance when the NDP and ABP were spun into PFs by melt spinning method at temperature of 335°C. Therefore, the results indicated that the spinnability of ABP had not been deteriorated even it consisted more oxygen, which was usually considered as impurity atom. This might be attributable to the homogenous components of ABP， as previously mentioned.

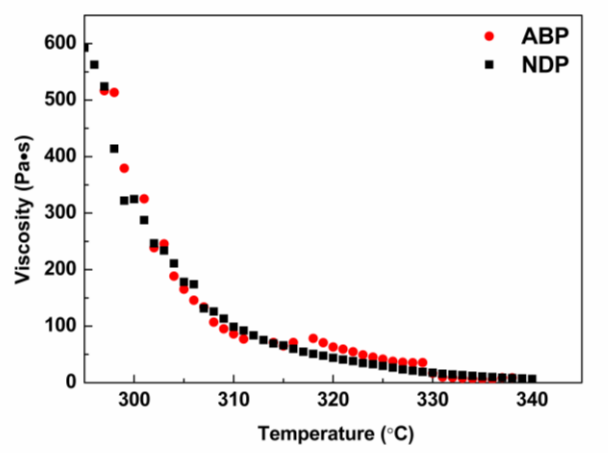

Fig. 5 Viscosity-temperature curves of NDP and ABP

3.3. Stabilization and carbonization of NDP-PF and ABP-PF

Stabilization is a crucial process to determine the properties of carbon fibers due to the formation of intermolecular cross-linking in an oxidizing atmosphere, which can ensure that the shape of fibers do not change in subsequent carbonization process [27]. Therefore, proper stabilization process should be adopted. In order to optimize the stabilization process, TG was used to measure the oxidation reactivity of fibers, as presented in Fig. 6. Lower initial temperature of weight gain indicated higher oxidation reactivity of ABP-PF than NDP-PF, which was proved by higher E_a and lower T_{max} of ABP-PF displayed in Table 3. Higher oxidation reactivity of ABP-PF may owe to lightest component remained in ABP instead of being removed like NDP by distillation at high temperature. However, the W_{max} in oxidation of ABP-PF was less than NDP-PF, which were 11.6% and 12.8% respectively, as exhibited in Table 3. This result could be interpreted as higher oxygen existed in ABP could restrain more oxygen from diffusing into fibers. This viewpoint could be demonstrated by similar oxygen content of NDP-SF and ABP-SF, as presented in Table 3.

Peer-reviewed version available at Materials 2019, 12, 305; doi:10.3390/ma12020305

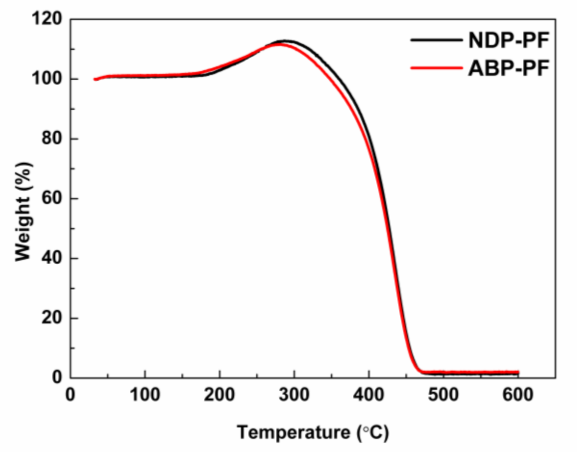

Fig. 6 TG curves of NDP-PF and ABP-PF

Table 3. Oxidation and carbonization properties of pitch fibers

Samples	T_{max} (°C)	W_{max} (%)	E_a (KJ/mol)	Oxygen content (%)	Yield (%)
NDP-SF	286	12.8	124.5	25.46	114.0
ABP-SF	278	11.6	120.5	25.72	112.5
NDP-CF	-	-	-	8.96	71.3
ABP-CF	-	-	-	10.29	71.0

T_{max}, W_{max} and E_a were calculated from TG results of NDP-PF and ABP-PF in air mood.

After 1200°C carbonization, both of NDP-CF and ABP-CF had high yield over 70%, which is favourable for producing low cost general purpose carbon fibers. Higher oxygen content of ABP-CF than NDP-CF shown in Table 3 denoted that less oxygen of ABP-CF given off during carbonization process in view of similar oxygen content of NDP-SF and ABP-SF. Less gas was released in carbonization process of ABP-SF (35.7%) than NDP-SF (37.7%), which might be beneficial to mechanical properties of CFs due to fewer defects would be generated. It also illustrated that the oxygen existed in pitch precursor was more stable than that introduced in stabilization process. This could be verified by the TG-MS results of NDP-SF and ABP-PF as shown in Fig 7(a) and 7(b), which were the CO and CO_2 from oxygen-containing group of fibers given off during carbonization process respectively. Both of CO and CO_2 were released at two stages, the first peak located between 400-800°C and 270-850°C, respectively. Then the amount of release began to increase rapidly for both CO and CO_2 especially for NDP-SF. It should be noted that the difference of the release amount of CO_2 for NDP-SF and ABP-PF was more distinct. The NDP-SF revealed higher peak intensity and magnitude of CO_2 in both two stages especially the high temperature stage than ABP-PF, which declared that the oxygen removal was more arduous below 1200°C when the oxygen introduced from the pitch precursor by air blowing than the oxygen introduced from the stabilization process. Therefore, the moderate amounts of oxygen in pitch precursor could improve the stabilization and carbonization properties of pitch fiber.

Peer-reviewed version available at Materials 2019, 12, 305; doi:10.3390/ma12020305

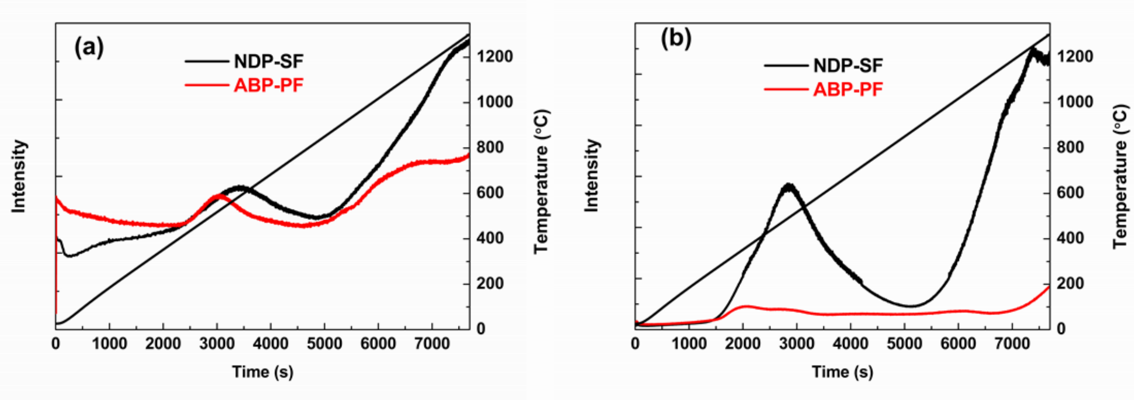

Fig. 7 MS curves of NDP-SF and ABP-PF (a) CO, (b) CO_2

3.3. Morphology and mechanical properties of NDP-CF and ABP-CF

The SEM micrographs of CFs were shown in Fig. 8. ABP-CF expressed more homogeneous and smooth surfaces and cross-sections than NDP-CF, corresponding to more homogeneous precursor pitch. Moreover, the fibers exhibited no fusing, indicating that the stabilization process had been adequate. The cross section of the CFs showed a glass-like fracture surface, indicating that the precursor pitch was isotropic. The tensile strength and modulus of CFs were presented in Fig. 9. ABP-CF had a tensile strength of 550 to 895 MPa and modulus of 31 to 45 GPa when the diameter decreased from 14.1 to 9.8 μm, always higher than NDP-CF, which was 448 to 748 MPa for tensile strength and 27 to 35 GPa for modulus as the diameter decreased from 13.1 to 8.7 μm. Both of the tensile strength decreased with increasing diameter. The mechanical properties reached the level of commercial general purpose CFs. Higher tensile strength should thanks to uniform composition of ABP and less gas released in carbonization which could produce defects in CFs due to the existence of oxygen as discussed previously. Whether the more oxygen which would be removed at higher temperature above 1200°C had an unfavorable effect on the properties of CFs need further investigation.

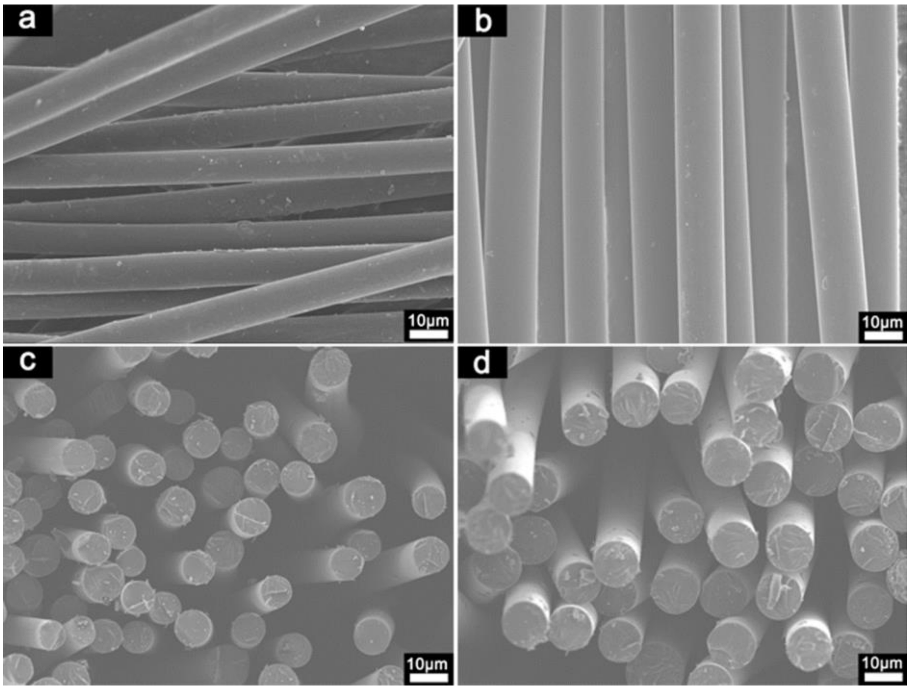

Fig. 8 SEM micrographs of (a, c) NDP-CF and (b, d) ABP-CF

Peer-reviewed version available at *Materials* **2019**, *12*, 305; doi:10.3390/ma12020305

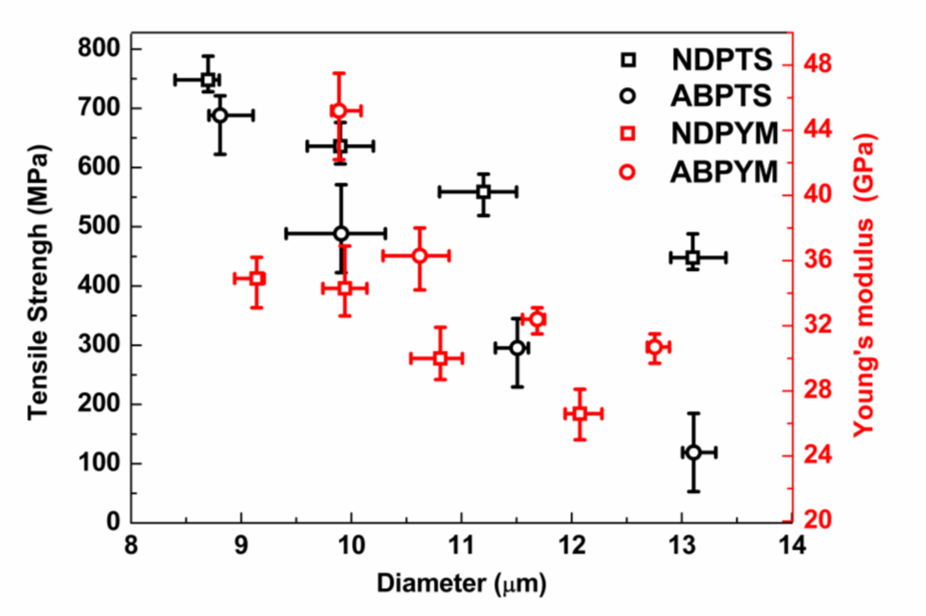

Fig. 9 The mechanical properties of NDP-CF and ABP-CF

4. Conclusions

Two isotropic pitches were prepared through atmospheric distillation and air blowing respectively. ABP had a higher yield and more homogeneous composition than NDP because oxygen could connect smaller molecules and suppress the ordered stack of larger molecules. The oxygen existed in pitch precursor was more difficult to be removed during carbonization, contributing to higher tensile strength of ABP-CF than NDP- CF. The tensile strength of ABF-CF and NDP-CF were 860 MPa and 640 MPa, respectively when the diameter was about 10μm, and the modulus were 41 GPa and 33 GPa, respectively. Thus, the present results revealed that the introduced oxygen from pitch precursor preparation process had significant difference comparing to that from pitch fiber stabilization process. And the evolution of introduce oxygen will be investigated in detail during the pitch precursor, stabilization and carbonization process in the future work.

Author Contributions: Conceptualization, J.Y. and X.L.; Methodology, K.S.; Validation, K.S., J.Y., C.Y., H.L. and K.S.; Formal analysis, K.S. and J.Y.; Investigation, K.S.; Data curation, K.S. J.Y. and X.L.; Writing—original draft preparation, K.S.; Writing—review and editing, J.Y. and X.L.; Supervision, H.L.; Project administration, X.L.; Funding acquisition, J.Y. and X.L.

Funding: Please add: This research was funded by (i) the Key Project of Chinese National Programs (2016YFB0101702), (ii) the National Science Foundation for Young Scientists of China (Grant No. 51702094), and (iii) the Natural Science Foundation for Young Scientists of Hunan Province, China (Grant No. 2017JJ3014).

Acknowledgments: The authors appreciate the support of Wuhan Luhua yueda chemical co. LTD, China for providing ET.

Conflicts of Interest: The authors declare no conflict of interest.

References

1. Frank, E.; Steudle, L. M.; Ingildeev, D. Carbon Fibers: Precursor Systems, Processing, Structure, and Properties. *Angew. Chem. Int. Ed.* **2014**, *53*, 5262-5298.
2. Mochida, I.; Toshima, H.; Korai, Y. Blending mesophase pitch to improve its properties as a precursor for carbon fibre I. Blending of PVC pitch into coal tar and petroleum-derived mesophase pitches. *J. Mater. Sci.* **1988**, *23*, 670-677.
3. Kim, B.; Eom, Y.; Kato, O. Preparation of carbon fibers with excellent mechanical properties from isotropic pitches. *Carbon* **2014**, *77*, 747-755.
4. Mora, E.; Blanco, C.; Prada, V. A study of pitch-based precursors for general purpose carbon fibers. *Carbon* **2002**, *40*, 2719-2725.

Peer-reviewed version available at *Materials* **2019**, *12*, 305; doi:10.3390/ma12020305

5. Xu, Y.; Chung, D. D. L. Silane-treated carbon fiber for reinforcing cement. *Carbon* **2001**, *39*, 1995-2001.
6. Fu, X.; Lu, W.; Chung, D. D. L. Ozone treatment of carbon fiber for reinforcing cement. *Carbon* **1998**, *36*, 1337-1345.
7. Chand, S. Review carbon fibers for composites. *J. Mater. Sci.* **2000**, *35*, 1303-1313.
8. Shirvanimoghaddam, K.; Hamim, S. U.; Karbalaei, A. M. Carbon fiber reinforced metal matrix composites: Fabrication processes and properties. *Compos. Part. A-Appl. S.* **2017**, *92*, 70-96.
9. Park, S. H.; Kim, C.; Choi, Y. O. Preparations of pitch-based CF/ACF webs by electrospinning. *Carbon* **2013**, *41*, 2655-2657.
10. Yang, J.; Nakabayashi, K.; Miyawaki, J. Preparation of pitch based carbon fibers using Hyper-coal as a raw material. *Carbon* **2016**, *106*, 28-36.
11. Kim, J. G.; Kim. J. H.; Song, B. Synthesis and its characterization of pitch from pyrolyzed fuel oil (PFO). *J. Ind. Eng. Chem.* **2016**, *36*, 293-297.
12. Barr, J. B.; Lewis, I. C. Chemical changes during the mild air oxidation of pitch. *Carbon* **1978**, *16*, 439-444.
13. Mochida, I. Inaba, T. Korai, Y. Carbonization properties of carbonaceous substances oxidized by air blowing-I: Carbonization behaviors and chemical structure of residual oils oxidized by air blowing. *Carbon* **1983**, *21*, 543-552.
14. Mochida, I. Inaba, T. Korai, Y. Carbonization properties of carbonaceous substances oxidized by air blowing-II: Acid-catalyzed modification of oxidized residual oil for better anisotropic development. *Carbon* **1983**, *21*, 553-558.
15. Blanco, C.; Santamar, A. R.; Bermejo, J. A comparative study of air-blown and thermally treated coal-tar pitches. *Carbon* **2000**, *38*, 517-523.
16. Menendez, R.; Blanco, C.; Santamaria, R. On the chemical composition of thermally treated coal-tar pitches. *Energ. Fuel.* **2001**, *15*, 214-223.
17. Prada, V.; Granda, M.; Bermejo, J. Preparation of novel pitches by tar air-blowing. *Carbon* **1999**, *37*, 97-106.
18. Maeda, T.; Zeng, S. M.; Tokumitsu, K. Preparation of isotropic pitch precursors for general purpose carbon fibers (GPCF) by air blowing-I. Preparation of spinnable isotropic pitch precursor from coal tar by air blowing. *Carbon* **1993**, *31*, 407-412.
19. Zeng, S. M.; Maeda, T. Tokumitsu, K. Preparation of isotropic pitch precursors for general purpose carbon fibers (GPCF) by air blowing-II. Air blowing of coal tar, hydrogenated coal tar, and petroleum pitches. *Carbon* **1993**, *31*, 413-419.
20. Fernández, J. J.; Figueiras, A.; Granda, M. Modification of coal-tar pitch by air-blowing-I. Variation of pitch composition and properties. *Carbon* **1995**, *33*, 295-307.
21. Fernández, A. L.; Granda, M.; Bermejo, J. Air-blowing of anthracene oil for carbon precursors. *Carbon* **2000**, *38*, 1315-1322.
22. Mishra, A.; Saha, M.; Bhatia, G. A comparative study on the development of pitch precursor for general-purpose carbon fibres. *J. Mater. Process. Tech.* **2005**, *168*, 316-320.
23. Wu, B.; Hu, H.; Zhao, Y. XPS analysis and combustibility of residues from two coals extraction with sub- and supercritical water. *J. Fuel. Chem. Technol.* **2009**, *37*, 385-392.
24. Matsumoto, T.; Mochida, I. A structural study on oxidative stabilization of mesophase pitch fibers derived from coal tar. *Carbon* **1992**, *30*, 1041-1046.
25. Andersen, S. I.; Jensen, J. O.; Speight, J. G. X-ray Diffraction of subfractions of petroleum asphaltenes. *Energ. Fuel.* **2005**, *19*, 2371-2377.
26. Korai, Y.; Mochida, I. Molecular assembly of mesophase and isotropic pitches at their fused states. *Carbon* **1992**, *30*, 1019-1024.
27. Drbohlav, J.; Stevenson, W. T. K. The oxidative stabilization and carbonization of a synthetic mesophase pitch, part I: The oxidative stabilization process. *Carbon* **1995**, *33*, 693-711.